IOSR Journal of Applied Chemistry (IOSR-JAC)
e-ISSN: 2278-5736.Volume 13, Issue 5 Ser. I (May. 2020), PP 01-10
www.iosrjournals.org

ESR Spectra Illuminate a Molecular Mechanism for Nickel(I) Catalysis of Ethylene Polymerization

M.K. Carter
Carter Technologies, Lincoln, CA 95648

Abstract:*ESR spectral measurements illuminated changes in a catalystduring formation of ethylene oligomersor polyethylene.A nickel(I) organic complex wasstudied under actual reaction conditions and at several temperatures showing changes related to catalyst structure that were unusually revealing of the details of catalysis, its degenerate electronic states and the associated mechanistic molecular reaction pathways.*
Keyword: *Nickel(i), ESR spectra, catalyst, polyethylene, molecular mechanism*

Date of Submission: 16-04-2020 Date of Acceptance: 01-05-2020

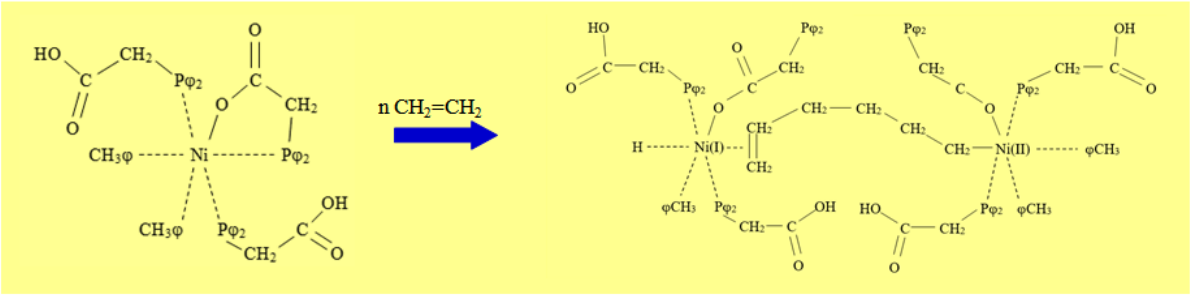

I. Introduction

Catalysis of a Ni(I) organometallic compound was studied in detail using ESR, TOF-MS, IR, NMR and UV spectroscopies,over a range of temperatures, showing changes in catalyst structure during oligomerization and polymerization of ethylene.As a result, the catalyst structure was elucidated and molecular reaction mechanisms have been proposed to illuminate the several shifts in equilibria with temperature as ethylene became oligomerized or polymerized, depending on the polarity of the solvent employed.

Catalysis has been defined[1] as a barrier free transformation from one electronic configuration to another, changing reactants to products. Further, the validity of this concept has been demonstrated in two detailed experimental efforts[2,3]. Catalysts have been supposed to not participate in chemical reactions and it has also been supposed that kinetics of catalytic reactions behave like typical chemical reactions. While this may be true in concept,the effect of vibronic distortion of the catalytic step as well as a requirement for degeneracy[1] in the electronic ground state energy of a catalyst have been overlooked. In addition, homogeneous and heterogeneous catalysts have been treated quite differently, although it is currently believed that the main difference between them is that a support acts like a π-bonded ligand that competeswithother ligands and solventsfor catalyst' sites.

The goals of this work are to illuminate the molecular structure of the catalyst during polymerization, to uncover the convoluted path of a catalytic process and to demonstrate the requirement of molecular symmetry, here D_{2h}, and its associated two-fold electronic degeneracy during polymerization reactions. This particular chemistry is subject to a 2 Ni(I) ↔ $[Ni(I)]_2$catalyst equilibrium.

II. Experimental Data

All data presented herein was collected some 50 years ago[4]. The catalyst compound was prepared in a 1 liter flask in the absence of air wherein a solution of 9.869 grams (0.0404 mol) of diphenylphosphine acetic acid in 400 mL dry toluene was added to a solution of 5.558 grams (0.0202 mol) of bis(cyclooctadiene)nickel(0) (nickel$(COD)_2$) in 270 mL of dry toluene with stirring at -1 to -2°C under dry argon. The reaction was completed in one hour as red-orange crystal platelets settled from solution. The crystals melted on warming to room temperature forming an insoluble red-brown oil. It was stirred continually for an additional two- and one-half days at 23°C as the red-brown oil slowly dissolved and a yellow-orange solid precipitated from solution. The mixture was filtered at 0°C under dry argon as a green colored solution passed through a dry sintered glass

filter. The yellow-orange solid was washed three times with dry toluene until no further green color was observed in the filtrate. The isolated solid identified as Nickel Orange was then dried under vacuum. The initial green filtrate solution was analyzed by GC wherein cyclooctene and cyclooctadienes were detected.

A time of flight mass spectrum (TOF-MS), measured for Nickel Orange, produced a value of 968 to 978 atomic mass units with individual atomic values detected for nickel, phosphorous, carbon, oxygen and hydrogen. This corresponded to the compound [diphenylphosphine acetic acid]$_2$Ni(diphenylphosphine acetate)[toluene]$_2$ with a molecular weight = 974.6 amu. A second TOF-MS measurement was conducted for the yellow-orange solid as it decomposed above 96°C that produced two mols of carbon dioxide and two mols of toluene per mol of starting material.

Proton NMR measurements were conducted on a Varian Associates model A-60 spectrometer at 50°C for toluene as -φ (φCH_3) at 7.18 δ (ppm) as well as for the ligand in acetone-$d_6$as -CH_3 ($\varphi_2PCH_2CO_2H$) at 0.99 (impurity), -CH_2- ($\varphi_2PCH_2CO_2H$) at 4.37, -Pφ_2 ($\varphi_2PCH_2CO_2H$) at 7.42, -CH_2D (solvent) at 2.02 (split by 0.04 into five sub-components) and -CD_3 (solvent) at 2.08. NMR measurements were performed for the Nickel Orange compound dissolved in acetone-d_6.Proton resonances were -CH_3 at 2.29, -φ at 7.11, -Pφ_2 at 7.52 and 7.78, -CH_2- at 6.0±0.2 broad and -CH_3 (φCH_3) at 2.30. The toluene methyl group indicated no shift, but the phenyl group was shifted up field by 0.07. Two diphenyl phosphine resonances were observed at 7.52, shifted by -0.10, and 7.78, shifted by -0.36. The solvent did exhibit H-D exchange with the acid ligand. This data lead to a structure for the Nickel Orange catalyst, refer to figure 1.

The bulk magnetic susceptibility of the dry solid measured at liquid nitrogen temperature was 1.76±0.22 Bohr Magnetons indicating there was one unpaired electron per molecule while the solution magnetic susceptibility was 0.0 Bohr Magnetons.

A second compound was prepared as before except the solvent was a 2:1 mixture of toluene and trifluoroethanol. This produced a nickel (1-bisphenylphosphine) acetate with associated trifluoroethanol plus byproducts of cyclooctadienes, bi-cyclooctadienes and a lesser amount of cyclooctene. An elemental analysis conducted for the isolated yellow-orange solid provided measured values of
Exp:$Ni_{1.0}O_{3.0}P_{1.1}C_{16.1}(H+F)_{17.2}$ that corresponded to theoretical values of
Theo:$Ni_{1.0}O_{3.0}P_{1.0}C_{16.0}(H+F)_{18.0}$. An infrared spectrum of the later nickel complex provided absorption bands at 1605 cm^{-1} for asymmetric nickel CO_2 stretch, 1380 cm^{-1} for symmetric nickel CO_2 stretch, 1465 cm^{-1} for the phenyl phosphorous group absorption and 720 to 680 cm^{-1} for monosubstituted aromatic rings.

Ethylene gas reactions were conducted using 0.10 gram of the Nickel Orange catalyst prepared from nickel (1-bisphenylphosphine) acetate in toluene with addition of organic additives to alter product average molecular weight and distribution. Resulting product information is presented in table 1.

A second set of ethylene reactions was conducted in a 100 mL water cooled reactor for a period of 0.5 to 2.0 hours. At the end of the reaction period the reaction pressure was vented (releasing mostly butenes and solvent vapor), weighed and opened. Solvent and volatiles below C_{20} were removed under vacuum leaving waxes C_{20} and greater. The liquid composition was determined by GC analysis and the wax content was determined by weight, refer to the data of table 2.

An ethylene reaction was also conducted in perdeuterated methanol for one hour and an NMR analysis found no un-deuterated methyl or alcohol group resonances indicating no D-H exchange. UV analysis of this catalyst product solution in methanol displayed an absorption maximum at 0.42 nm for the nickel complex as compared with an absorption maximum at 0.40nm for the un-reacted nickel complex in toluene.

Table 1. Effect of Additives on Product Formation

Additive *	Pressure (psig)	Temperature (°C)	Average Reaction Rate (g prod/g Ni/hr) **	Products
s-trichlorophenol	620	60	1,500	C_4 to C_{20}
cyanuric acid	700	65	2,400	C_4 to C_{20} w. some branching
φ-$C(CF_3)_2$-OH	600	70	1,200	mostly C_4 to C_8
0.1 g $SnSO_4$	900	70	1,000	polyethylene + oligomer
sulfolane	560	80	90	C_4 to C_{20}
methyl phenyl ether	960	75	1,000	C_4 to C_{20}
p-dichlorobenzene	800	74	1,600	C_4 to C_{20}
benzaldehyde	950	70	0	catalyst oxidized
water	500	65	200 (reaction stopped after 10 minutes)	oligomers and waxes

* Propene, butenes and hexanes also formed oligomeric products.
** Butenes were vented and not included in rate determinations.

Table 2. Effect of Solvents on Product Formation

Co-solvent	Average Pressure (psig)	Temperature (°C)	Reaction Rate (g product/g Ni/hr)	Products
2-ethylhexanol	700	80	3,510	14% wax
decanol	700	80	1,850	oligomers
t-butanol	700	80	2,960	4% wax
CH_3NO_2	700	80	0	catalyst oxidized
n-$C_{15}OH$	650	75	1,260	32% wax
CD_3OD	550	75	1,910	oligomers
DMF	400	70	300	polymer
C_6F_6	400	70	300	polymer
hexanes	---	---	---	Polymer
CF_3CH_2OH	250	70	3,010	oligomers
n-butanol	775	69	4,500	75% wax

A separate set of measurements was conducted relating ethylene reaction rate to the number of paramagnetic centers present. Results are presented in table 3.

Table 3. Reaction Rate vs Number of Paramagnetic Centers

Paramagnetic Centers (number/10^4 Ni molecules)	Reaction Rate (grams product/grams Ni/hour)
2	19
18	97
38	168

Anisotropic ESR spectrawere recorded on a Varian Associates model V-4500 x-band, modified, using the dual cavity operation in the HE_{104} mode with tetracene cation radical as the g-value standard for g = 2.002598 and manganese (2+) as the splitting standard for a(average) = 95.0 gauss.Anisotropic ESR spectra of the solid Nickel Orange complex at 23°C accounted for 1 unpaired electron per 100 Nickel Orange molecules (refer to figure 2) whereas an anisotropic ESR spectrum of a methanol solution of the compound at 77K accounted for 1 unpaired electron per 3 molecules. This corresponded with a decrease in the intensity of an ESR spectra as temperature increased. An ESR spectrum of a methanol solution of Nickel Orange in a glassy solid state at -138°C (refer to figure 3) exhibited four $g_{\|}$ lines with intensity ratios of 1:3:3:1 indicating three spin ½ phosphorous atoms were associated with the nickel atom and a single $g_{\perp}$ line with indications of further splitting in some spectra. A partially resolved ESR spectrum recorded as the temperature was increased to -92°C (refer to figure 4) showed five $g_{\|}$ lines with intensity ratios of approximately 15:20:15 for the three more intense lines indicating four spin ½ phosphorous atoms were associated with the nickel atom and a single broad $g_{\perp}$ line indicating overlap of multiple contributions. A 0.4 gram sample of dry solid Nickel Orange was placed in 1 cm diameterSuper Sil ESR sample tube under dry argon and an anisotropic spectrum

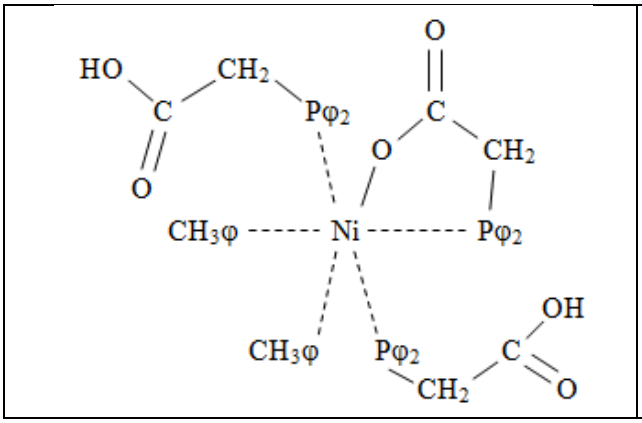

Figure 1. Molecular Structure of Nickel Orange

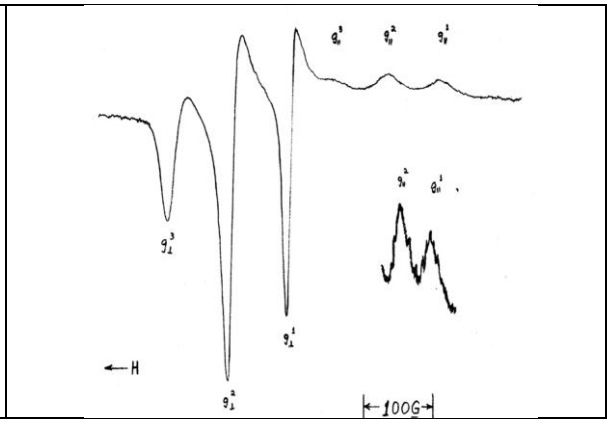

Figure 2. ESR Spectrum of Nickel Orange at 23°C

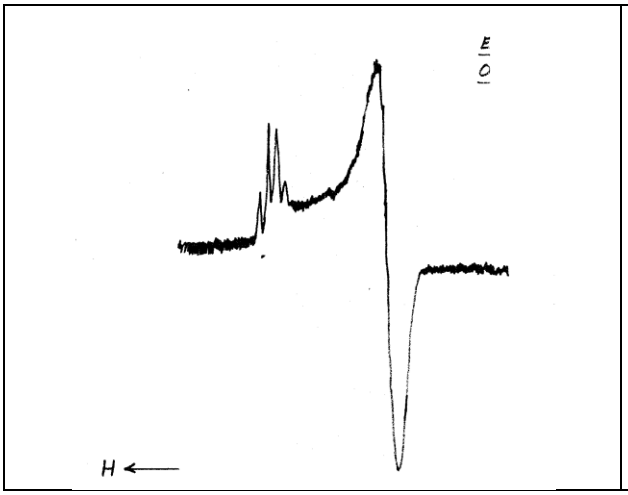

Figure 3. Nickel Orange in Methanol at – 138°C

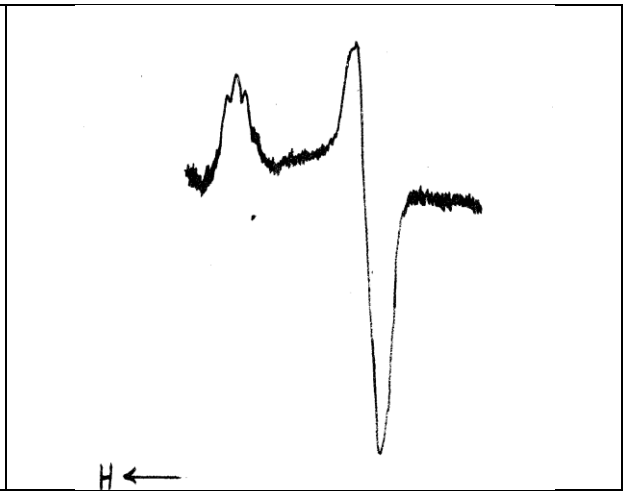

Figure 4. Nickel Orange in Methanol at – 92°C

recorded at 23°C exhibitingthree $g_{\|}$ lines plus three $g_{\perp}$ lines as presented in figure 2. The down field $g_{\|}$ lines were further resolved into five hyperfine lines split by approximately 12 gauss as presented in table 4.

Table 4. Spectroscopic Splitting Factors and Hyperfine Line Values of Figure 2

Spectroscopic Splitting Factors	Fine Line Splitting (gauss)	Hyperfine Line Splitting (gauss)
$g_{\|}^{1} = 2.2449$		
$g_{\|}^{2} = 2.1897$	$A_{\|}^{1\text{-}2} = 74.71$	$\langle A_{\|}^{1} \rangle^{1} = 11.4$
$g_{\|}^{3} = 2.1330$	$A_{\|}^{2\text{-}3} = 76.74$	$\langle A_{\|}^{2} \rangle^{2} = 12.9$
$g_{\perp}^{1} = 2.0860$, line width = 30 gauss		
$g_{\perp}^{2} = 2.0291$, line width = 22 gauss	$A_{\perp}^{1\text{-}2} = 92.35$	
$g_{\perp}^{3} = 1.9707$, line width = 17 gauss	$A_{\perp}^{2\text{-}3} = 94.82$	

The sample tube was evacuated and ethylene gas was introduced over a period of 7 days at a pressure of 30 psig. A comparatively large quantity of ethylene gas was absorbed as the original spectrum decayed and a new spectrum appeared, refer to figure 5. Not only was the spectrum different but it was immediately apparent the orientation of the spectrum was reversed compared to figure 3 in that the three $g_{\|}$ lines were up field (to the left) where the three $g_{\perp}$ lines resided in the previous spectrum,

Table 5. Spectroscopic Splitting Factors and Hyperfine Line Values of Figure 5

Spectroscopic Splitting Factors	
$g_{\perp} = 2.0549$, line width = 82 gauss	---
$g_{\|}^{1} = 1.6150$	---
$g_{\|}^{2} = 1.5034$	$A_{\|}^{1\text{-}2} = 33.4$
$g_{\|}^{3} = 1.4149$	$A_{\|}^{2\text{-}3} = 32.8$

refer to spectral data of table 5. The width of the $g_{\perp}$ line was 82 gauss indicating that multiple unresolved lines were present. In addition, remnants of the original three $g_{\perp}$ lines were still present indicating species of two different molecular structures. The new spectrum of figure 5, present at approximately 60 percent of the intensity of the original spectrum, exhibited three $g_{\|}$ lines in intensity ratios of 1:2:1 indicating two phosphines groups were associated with the nickel atom. The same experiment was conducted using perdeuterated ethylene gas and an identical ESR spectrum was recorded.

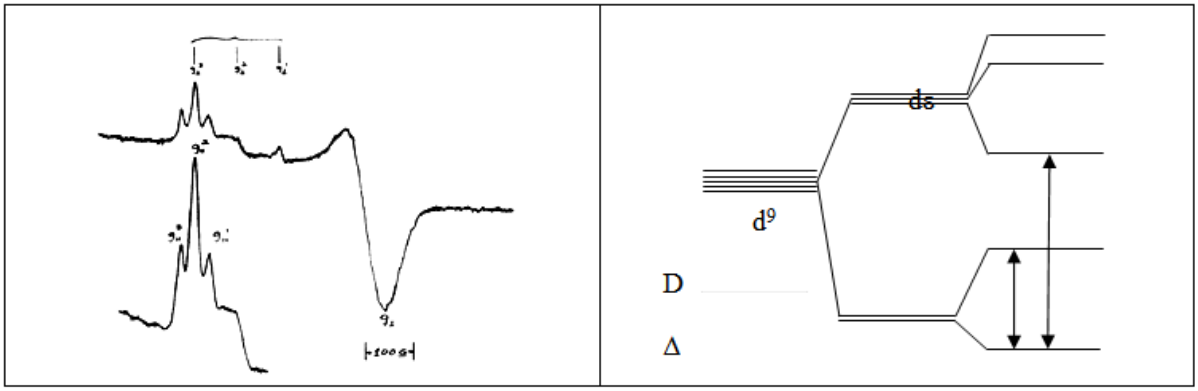

Figure 5. ESR Spectrum of Nickel Orange Catalyst Figure 6. Perturbation by a Cubic Octahedral During Ethylene Polymerization Crystal Field Producing d^9 Splitting

Upon completion of the spectral measurements the sample tube was opened, weighed to show the solid weight had doubled to 0.8 gram, extracted with dry n-hexane to remove the oligomers then extracted with dilute hydrochloric acid for several hours to dissolve the nickel catalyst. The remaining solid was low density polyethylene as identified by its IR spectrum.

A residual hydrocarbon wax sample from table 2 was analyzed by NMR to determine the end groups present. There were resonance lines for a vinyl group, two types of methylene groups and a methyl group. One type of methylene group, assumed to be adjacent to a vinyl group, was measured as distinct from the more intense molecular back bone methylene groups. The relative intensity ratios for the vinyl group, the methylene group adjacent to the vinyl group and the methyl group were 1:1:1.

UV spectra were recorded for Nickel Orange samples dissolved in dry methanol under argon gas and compared with methanol solutions of diphenylphosphine acetic acid and toluene. Nickel Orange dissolved in dry methanol exhibited an absorption shoulder shifted to 0.30nm. The solvent was removed at 85°C under high vacuum, the solid was re-dissolved in dry methanol and another UV spectrum recorded displaying the shoulder at 0.30nm with reduced intensity. The ligand solution exhibited characteristic aromatic absorption in the 0.24mto 0.27nm region while toluene exhibited similar absorption in the 0.25nm to 0.28nm range.

III. Discussion

A nickel diphenylphosphine acetate compound was prepared that was quite active as a catalyst for ethylene oligomerization to α-olefins in a solvent[5] and for formation of polyethylene in thenon-solvent hexane or as a dry solid[6]. In addition, catalytic activity was associated with the number of paramagnetic centers, refer to data presented in table 3. Chemical reaction ofbis(cyclooctadiene)nickel(0) with diphenylphosphine acetic acid, both dissolved in toluene at 0°C in the absence of air, produced three main products as a result of a chemical reaction equilibrium. The products were (a) Ni(II) (diphenylphosphine acetate)$_2$ a green compound, (b) [diphenylphosphine acetic acid]$_2$ Ni(II) (diphenylphosphine acetate)$_2$ and (c) [diphenylphosphine acetic acid]$_2$ Ni(I) (diphenylphosphine acetate) a yellow-orange compound identified as Nickel Orange leaving some of the bis(cyclooctadiene)nickel(0) complex un-reacted.

GC analysis of the initial green filtrate solution, that remained after yellow-orange solids had been isolated, identified the presence of cyclooctene and cyclooctadienes. Cyclooctene most likely formed by partial hydrogenation of cyclooctadiene from hydrogen released as the acetic acid ligand formed a nickel acetate bond. A TOF-MS measurement for the dry Nickel Orange solid produced a value of 968 to 978 atomic mass units with individual atomic values detected for nickel, phosphorous, carbon, oxygen and hydrogen that corresponded to the compound [diphenylphosphine acetic acid]$_2$Ni(diphenylphosphine acetate)[toluene]$_2$ with a molecular weight = 974.6 amu. A second TOF-MS measurement was conducted for the yellow-orange solid at a temperature above 96°C demonstrating decomposition to two mols of carbon dioxide and two mols of toluene per mol of starting material.This indicated that two mols of diphenylphosphine acetic acid and two mols of toluene were originally part of the Nickel Orange compound bonded as π-bonded ligands. Based on this information a representative molecular structure for Nickel Orange is presented in figure 1,

Proton NMR measurements conducted for the ligand dissolved in acetone-$d_6$produced proton resonances measured in δ (ppm). A methyl impurity resonance ($\varphi_2PCH_2CO_2H$) was recorded at 0.99, the ligand methylene ($\varphi_2PCH_2CO_2H$) at 4.37 and the diphenyl phosphine ($\varphi_2PCH_2CO_2H$) at 7.42. The solvent-CH_2D was recorded at 2.02 as split by 0.04 into five sub-components and a solvent -CD_3 at 2.08. The solvent exhibited H-D exchange with the acid ligand indicating that some of the acid groups were not bonded to the nickel atom. Proton NMR measurements were conducted for the Nickel Orange compound dissolved in acetone-$d_6$at 50°C.

Proton resonances were measured for $-CH_3$ at 2.29 and -φ at 7.18 identifying the toluene ligands. Two diphenyl phosphine resonances were observed at 7.52 shifted by-0.10 and 7.78 shifted by -0.36 that indicated two different types of biphenyl phosphine groups were bonded to the nickel atom, two at 7.52 and one at 7.78[7]. A broad methylene resonance recorded at 6.0±0.2 was likely the ligand σ-bonded to the nickel atom broadened by contribution of unpaired electron character. The toluene methyl group indicated no shift, but the phenyl group was shifted up field by 0.07 indicating its association with the nickel complex.

An elemental analysis of the yellow-orange solid nickel bis-phenylphosphine acetate formed in a 2:1 solvent mixture of toluene and trifluoroethanol provided elemental analysis values of
Exp: $Ni_{1.0}O_{3.0}P_{1.1}C_{16.1}$ $(H+F)_{17.2}$ that corresponded to theoretical values of
Theo: $Ni_{1.0}O_{3.0}P_{1.0}C_{16.0}$ $(H+F)_{18.0}$. This data was accepted to be in reasonable agreement.

An infrared spectrum of this nickel complex provided absorption bands at 1605 cm^{-1} for asymmetric nickel CO_2 stretch, 1380 cm^{-1} for symmetric nickel CO_2 stretch, 1465 cm^{-1} for the phenyl phosphorous group absorption and 720 to 680 cm^{-1} for monosubstituted aromatic rings. A large number of phenyl phosphine compounds exhibit absorption in the 1425 to 1450 cm^{-1} range[8]indicating the shift to 1465 cm^{-1} was a result of a diphenyl phosphine π-bonding with the nickel atom. Bonding for the diphenylphosphine ligand was the same as that for Nickel Orange. Other nickel phosphine compounds have been reported that were also effective for oligomerization of ethylene[9].

ESR spectra and supporting TOF-MS, IR, NMR and UV spectra produced unusually detailed data elucidating the structure and a molecular mechanism for nickel (I) catalysis during ethylene oligomerization. A set of catalytic ethylene oligomerization reactions was conducted demonstrating the reaction rate was a function of the concentration of paramagnetic centers as presented in table 3 confirming that the catalyst was paramagnetic. An ESR spectrum of solid Nickel Orange recorded at 23°C in dry argon was anisotropic exhibiting three $g_{\|}$ lines and three $g_{\perp}$ lines as presented in figure 2. The down field $g_{\|}$ lines were each further resolved into five hyperfine lines split by approximately 12 gauss as presented in table 4 indicating four spin ½ phosphorous atoms to be associated with the paramagnetic center. Since there are at most three phosphine groups bonded to each nickel atom this spectrum indicated formation of some type of molecular dimer association. The intensity of the spectrum accounted for one unpaired electron per 100 Nickel Orange molecules at 23°C whereas an ESR spectrum of a methanol solution of the compound at liquid nitrogen temperature of -196°C (77K) accounted for 1 unpaired electron per 3 molecules demonstrating an increase in the intensity of the ESR spectrum as temperature decreased. An ESR spectrum of a methanol solution of Nickel Orange in a glassy solid state at -138°C, as presented in figure 3, exhibited four $g_{\|}$ lines with intensity ratios of 1:3:3:1 indicating that at this temperature three spin ½ phosphorous atoms, $\Sigma_i I_i = 3/2$ so that $2I+1 = 4$, were associated with the nickel atom and a single broad $g_{\perp}$ line presented indications of further splitting in some spectra. Thus, the phosphine end of the σ-bonded ligand was π-bonded to the nickel atom as were the two associated phosphine ligands as shown in the molecular structure of figure 1. A partially resolved ESR spectrum recorded as the temperature was increased to -92°C showed five $g_{\|}$ lines with intensity ratios of approximately 15:20:15 for the three more intense lines indicating four nuclear spin ½ phosphorous atoms,
$\Sigma_i I_i = 2$ with $2I+1 = 5$, were associated with the nickel atoms and a single broad $g_{\perp}$ line indicated overlap of multiple contributions, refer to figure 4. These ESR spectra documented significant changes in the structure of the nickel(I) molecular complex with temperature.

The changes in the ESR spectrum have been interpreted as an equilibrium shift from isolated nickel (I) complex molecules to pairs of complex nickel (I) molecules. Since Nickel Orange may be shown to be a six coordinate nickel complex then pairing of two such molecules can be accomplished by rotating the phosphine ends of the σ-bonded ligands on each of the paired nickel complexes out of the nickel-nickel bond region producing the dimer similar to that shown in figure 7. This spectral data has been interpreted to indicate that Nickel Orange exists in a 2 monomer ↔1 dimer equilibrium. The nickel catalyst complex participates in several structural changes with temperature. The bulk magnetic susceptibility was measured for the dry Nickel Orange solid at liquid nitrogen temperature as 1.76±0.22 Bohr Magnetons indicating there was one unpaired electron per nickel (I) organometallic molecule for this $3d^9$ electron configuration while the solution magnetic susceptibility at room temperature was 0.0 Bohr Magnetons. For comparison, the bulk magnetic susceptibility reported for $Ni(II)(C_{16}H_{16}N_6S_2)Cl_2$ is $\mu = 2.89$[10] indicating two unpaired electrons per nickel atom for this $3d^8$ electron configuration.

ESR signal intensity of Nickel Orange dissolved in methanol changed exponentially with temperature. Attemperatures approaching -196°C (77K) the signal intensity increased to one unpaired electron per three nickel organic molecules. At the melting point of methanol, -97°C, the signal intensity measured one in seven and at 23°C it decreased to approximately one per hundred molecules. Apparently, the nickel (I) dimer

molecular complex, which is assumed to be nearly planar, can electron spin align with a second such complex in a spin coupled association as temperature increases resulting in four unpaired electron spins that add to zero net spin. Such spin aligned complexes would be disrupted by increasing organization of the methanol solvent molecules as the crystallization point and lower temperature crystal modifications are attained. ESR spectra have also been reported for nickel complexes in natural biological materials[11] indicating the unpaired electron character is also found in natural enzymes (natures catalysts).

The molecular structure of Nickel Orange was determined by NMR and a TOF-MS measured value of 968 to 978 amu that corresponded to the compound [diphenylphosphine acetic acid]$_2$Ni(diphenylphosphine acetate)[toluene]$_2$ with a molecular weight = 974.6 amu, however no data was measured for double the mass in the range of 1,950 amu at that time. Further, a bulk magnetic susceptibility of the dry solid measured at liquid nitrogen temperature was 1.76±0.22 Bohr Magnetons indicating there was one unpaired electron per nickel molecule complex. Monomeric nickel (I) compounds possess a single unpaired electron in a d^9 electron configuration $\Sigma_i S_i = 1/2$ such that for 2S+1 = 2 a doublet ESR spectrum that was anticipated as reported for Ni(COD)$_2$/BF$_3$-OEt$_2$[12]. Thus, it is apparent that the Nickel Orange complex possessed two unpaired electrons such that $\Sigma_i S_i = 1$ for 2S+1 = 3 indicating three lines as observed in the ESR spectrum of figure 2. Binuclear Ni-Ni compounds have been reported[13]with nickel-nickel bond distances of 232 pm to 279 pm while natural enzymes, that are known to catalyze chemical change, possess longer metal-metal bond distances in the region of

340pm[14,15]. This distance is sufficiently long such that two unpaired electron spins do not spin pair in formation of a singlet, rather they may exist in a natural low energy triplet state much like molecular oxygen. It is evident that the ESR spectrum of figure 2 represents a pair of Nickel Orange molecules with a nickel(I)-nickel(I) triplet electron configuration.

The down field $g_{\|}$ lines of figure 2 were further resolved into five hyperfine lines each split by approximately 12 gauss as presented in table 4. This spectral structure indicated the presence of four similar spin ½ nuclei bonded to the nickel atoms. The ESR spectrum of figure 4 related to the chemical bonding of a nickel(I)-nickel(I) dimer with two phosphine groups π-bonded to each of the nickel atoms as presented in figure 7 leaving the phosphine ends of the σ-bonded diphenylphosphine acetate ligands extended.

The dry Nickel Orange solid in the 1 cm Super Sil ESR sample tube mounted in the microwave detector of the ESR spectrometer was evacuated and ethylene gas was introduced over a period of 7 days at a pressure of 30 psig. A comparatively large quantity of ethylene gas was absorbed as the original spectrum decayed and a new spectrum appeared, refer to figure 5. Not only is the spectrum different from that of figure 2 but it is immediately apparent the orientation of the spectrum had been reversed in that the three $g_{\|}$ lines were up field (to the left) where the three $g_{\perp}$ lines resided in the previous spectrum (as indicated by residual $g_{\perp}$ lines of figure 2 as indicated in figure 5), refer to the data of table 5. The width of the $g_{\perp}$ line was 82 gauss indicating that multiple unresolved lines were present. In addition, remnants of the original three $g_{\perp}$ lines were still present indicating species of two different molecular structures were present at the same time. Such a reversal of spectrum orientation indicates that the nickel complex had been perturbed such that two nearly degenerate energy levels had been inverted. This perturbation is anticipated to be in the form of a change in geometrical structure of the catalytic complex. The new spectrum of figure 5, present at approximately 60 percent of the intensity of the original spectrum, exhibited three $g_{\|}$ lines in intensity ratios of 1:2:1 indicating only two phosphines groups were associated with each nickel atom. Apparently, association of ethylene with the nickel atom shielded the second nickel atom of the dimer complex indicating the catalyst in action. Paramagnetic transition metal compounds that exhibit spectral characteristics of an anisotropic crystal may be treated using a Hamiltonian operator perturbed by a crystal field, in this case by a cubic octahedral field as represented by the energy diagram in figure 6.

D-term splitting by a cubic octahedral field, representative of a d^9 electronic configuration, usually arises from electronegative species. Such tetragonal symmetry leaves axial $g_z = g_{\|} \neq g_x = g_y = g_{\perp}$ resulting from spin-orbit coupling that is mostly quenched or removed by the crystal field. This near balance of forces leaves the lowest occupied energy levels of a ground electronic state to be essentially degenerate.

The Hamiltonian describing paramagnetic resonance including fine and hyperfine splitting of an anisotropic system of axial symmetry has been expressed assuming a strong field, neglecting the effects of fine splitting (zero-field splitting) and the nuclear electric quadrapole moment[16], both of which are small. Then, invoking these simplifications, resonances occur to a second order at an energy expressed as

$$\Delta E = g\beta H_0 + Km_I + (A_{\perp}^2/4g\beta H_0)[(A_{\|}^2 + K^2)/K^2][I(I+1) - m_I^2]$$
$$+ (A_{\perp}^2/2g\beta H_0)(A_{\|}/K)(2|m_s| - 1)m_I + (1/2g\beta H_0)[(A_{\|}^2 - A_{\perp}^2)/K]^2(g_{\|}g_{\perp}/g^2)^2 m_I^2 \sin^2\theta\cos^2\theta$$

for which $K^2g^2 = A_{||}^2g_{||}^2\cos^2\theta + A_{\perp}^2g_{\perp}^2\sin^2\theta$ and $g^2 = g_{||}^2\cos^2\theta + g_{\perp}^2\sin^2\theta$. Assumptions for this crystal field model computation included $g_{||} = (1 - \lambda\Lambda_{||})$, $g_{\perp} = (1 - \lambda\Lambda_{\perp})$, $D = \lambda^2(\Lambda_{\perp} - \Lambda_{||})$ or $D \sim (\lambda^2/\Delta)$. Experimental spectroscopic values were $g_{||} = 1.5034$, $g_{\perp} = 2.0549$, $A_{||} = 33$ gauss and $A_{\perp} = 60$ gauss, refer to table 5. An average line width of 22 gauss was found to be consistent with these spectra so that the center to center line spacing was determined to be 60 gauss. Units considerations required that the Bohr magneton $\beta = 9.27408\text{x}10^{-24}$ (J/T) = $5.78839\text{x}10^{-4}$ (eV/T) where $1\text{x}10^4$ gauss = 1 T (Tesla). The energy computed for separation of these two essentially degenerate levels using the experimental data of table 5 is $\Delta E = 1.5$ kcal/mol (6.3 kJ/mol, 0.067 eV). Thus, the working catalyst is essentially in a degenerate state as perturbed by deviation from D_{2h} symmetry and a vibronic distortion possibly resulting from theon-going ethylene oligomerization reaction processes. Catalysts have been shown[1] to be active for a limited number of symmetric groups including C_{4v}, D_{4h} and D_{2h} each of which includes at least two-fold degenerate representation. This symmetry applies to the nickel atom and only those atoms directly bonded thereto since all other atoms are farther away and do not directly influence the electronic structure of the nickel atom as represented by the ESR spectrum. The dimer of Nickel Orange shown in figure 8 is close to D_{2h} symmetry (aromatic ring, phosphorous and oxygen atoms act as electronically similar) but does not strictly conform to this point group symmetry.

A second sample tube containing the same amount of Nickel Orange was placed in the ESR spectrometer, the same experiment was conducted at 23°C using perdeuterated ethylene gas and an identical ESR spectrum was recorded. This result confirmed that neither π-bonded ethylene nor growing oligomeric hydrocarbon chains were directly detected by this experimental measurement, but the presence of ethylene did cause the spectrum of the nickel complex to change. Upon completion of the spectral measurements the sample tube was shown to contain oligomers and low-density polyethylene, refer to the experimental section.

A residual hydrocarbon wax sample was analyzed by NMR to determine that one end of the oligomeric wax chain was a vinyl group with its adjacent methylene group and the other end was capped by a methyl group, refer to the experimental section. Apparently, an intermediate nickel hydride bond had formed making the hydrogen atom available at chain termination. Such a nickel hydride must be a short-lived intermediate state since it was not identified in either an IR spectrum or an NMR spectrum. The time of a molecular vibration is known to be quite short (the order of 10^{-12} second) and since the time for a polymer chain to grow under 20 to 30 pounds of ethylene gas pressure is assumed to be a sequence of such vibrations, then it may be concluded that the time for a polyethylene molecule to grow, even to a molecular weight of several million, could be less than a microsecond. It may be concluded that formation of a nickel hydride bond would not be detected under the experimental conditions. Clearly chain initiation requires transfer of a hydrogen atom to another location, be it taken by an alkene, another hydrogen atom or a nickel site, and chain termination requires reacquisition of a hydrogen atom. The only reacquisition energy that is sufficiently low to be practical is release of a hydrogen atom by a nickel hydrogen compound. Nickel hydride material has been prepared, measured by laser-induced fluorescence (LIF) excitation spectroscopy and confirmed as NiH recorded in the spectral region from 15,000 cm^{-1} to 21,400 cm^{-1}, for which NiH molecules were produced by the reaction of sputtered nickel atoms with methanol under supersonic jet conditions[17].

Consider how chain termination may occur. There are three types of termination reactions considered here. First there is (1) vibronic distortion of the nickel complex whereby its near D_{2h} symmetry is significantly distorted or broken during a vibronic perturbation. This is a function of its entire electronic density distribution, is related to the particular transition metal present and the states of its near degenerate levels causing rejection of the growing polymer chain. A second mode of termination is (2) due to a concerted vibrational distortion of the growing chain whereby it rips itself loose from the transition metal site. A third mode of termination is (3) observed for a catalytic complex in the presence of a polar solvent whereby a solvent molecule becomes associated with a transitional metal site concomitantly becomes

π-bonded and its electron donation contribution to the nickel molecular complex causes displacement of the growing chain. This mode may be observed to mitigate or reduce the average chain length from polymer to that of an oligomer. A pictorial representation of the proposed ethylene oligomerization or polymerization mechanism is represented by a sequence of molecular structure changes as follows. A monomer-dimer equilibrium is represented by figures 1 and 7 for which the diphenyl phosphine portion of the acetate ligand has rotated out of the nickel-nickel bond region. The dimer geometric configuration is similar to a resting state that becomes the catalyst as ethylene monomer becomes available.

Polymer chain initiation and propagation are represented by figures 8 through 11. This model sequence demonstrates a proposed molecular mechanism of how a catalyst performs its molecular catalytic functions while essentially complying with the requirements of symmetry being in a nearly degenerate electronic energy state. The presence of an abundance of ethylene monomer displaces the π-bonded toluene molecules as ethylene becomesπ-bonded to the nickel atom as represented in figure 8. This may be denoted as monomer capture. During a brief vibronic distortion (the order of 10^{-12} second)the nickel atom contributes an electron to form a nickel(II)ethyl σ-bond leaving the extra hydrogen atomto bond to the adjacent nickel atom of the dimer.

Refer to figure 9. These geometric structures havebeen presented here in two dimensions, however in three dimensions the growing oligomeric chain and

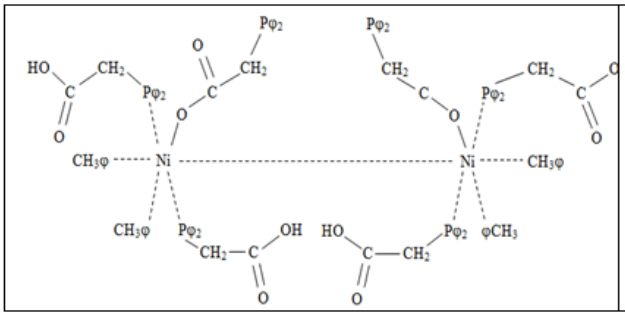

Figure 7. Nickel (I) Dimer with Four π-Bonded Toluene Molecules

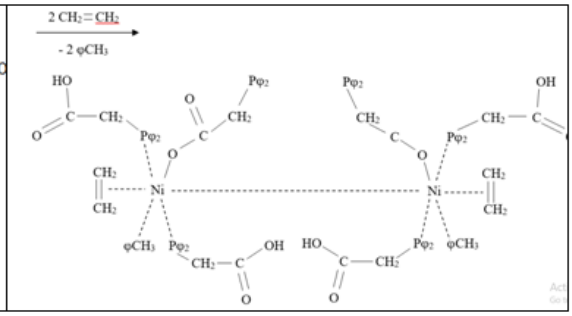

Figure 8. Nickel (I) Dimer with Twoπ-Bonded Ethylene Groups

nickel hydrogenare anticipated to be adjacent one to the other rather than opposed as shown. As the

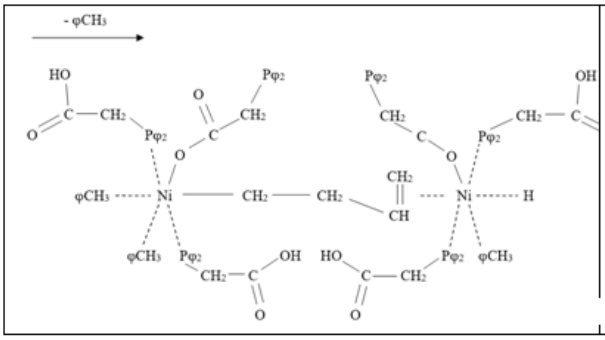

Figure 9. Nickel (I) Dimer with π-Bonded and σ-Bonded Butylene Group

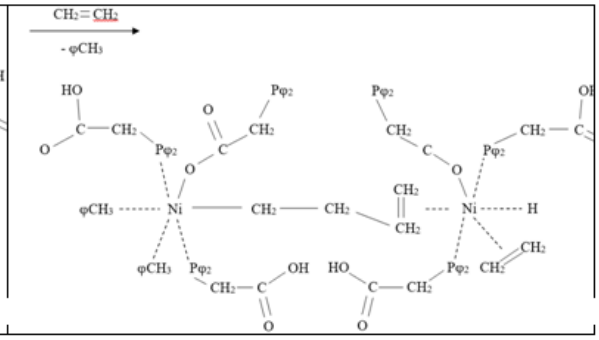

Figure 10. Nickel (I) Dimer with π-Bonded Ethylene and σ-Bonded Butylene Group

molecular conditions dictate, whether by solvent participation, monomer availability or the natural time for a vibronic distortion of the catalyst molecule, chain growth terminates as the contiguous hydrogen caps the σ-bonded carbon atom to become a methyl group. The void catalytic sites become occupied by π-bonded toluene solvent molecules, as before initial ethylene absorption, as represented by figure 7, unless another

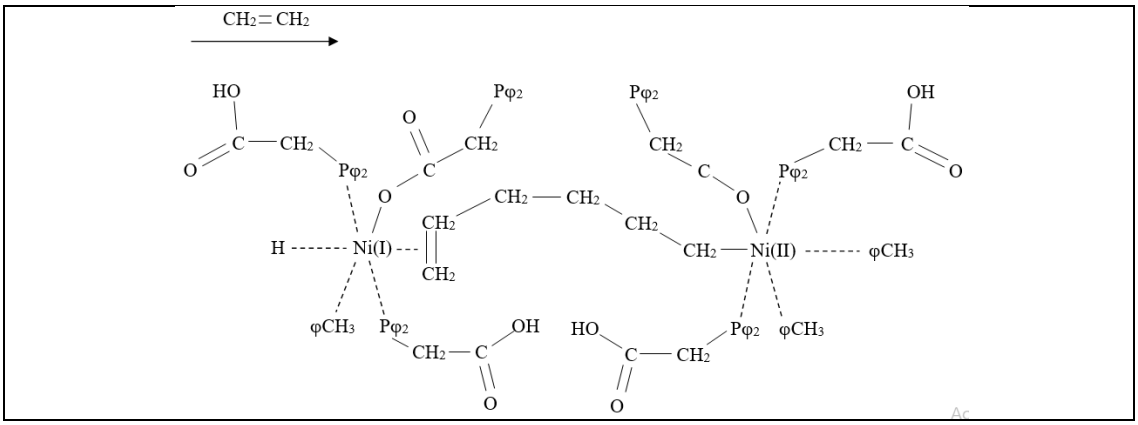

Figure 11. Nickel (I) Dimer with π-Bonded and σ-Bonded Hexylene Group

growingchain is initiated. An oligomerization reaction was also conducted in perdeuterated methanol and an NMR analysis found no un-deuterated methyl or alcohol group resonances indicating no D-H exchange had occurred during the reaction. In addition, UV analysis of the catalyst solution in methanol displayed an absorption maximum at 0.42nm for the nickel complex as compared with an absorption maximum at 0.40nm for the nickel complex in toluene indicating the polar solvent displaced toluene to become associated with the nickel complex. High Molecular weight polyethylene was formed in the presence of the non-solvent's hexane,

hexafluorobenzene and dimethylformamide while lower molecular weight oligomers were formed in the presence of ethers and alcohols capable of competing with π-complexes on the nickel atom similar to those of phosphine ligands. It is apparent that additives did displace or compete with ethylene chain initiation, chain termination perturbations and directed the type of products produced. It is also apparent that an electronic effect was produced by the apparent electron donor pair contribution of the perturbing additives or π-complexes. Waxes were produced by most of the alcohol solvents while liquid oligomers, mostly α-olefins, formed in the presence of the more active perturbing solvents s-trichlorophenol, cyanuric acid, hexafluoropropyl phenyl alcohol, sulfolane, methyl phenyl ether and p-dichlorobenzene.

IV. Conclusion

ESR spectral measurements, as supported by TOF-MS, NMR, IR and UV spectral data, conducted some 50 years ago[4] for a nickel (I) complex identified as Nickel Orange were instrumental in illuminating the molecular reaction path of catalysis for ethylene oligomerization and polymerization. In addition, the measurements revealed the ground electronic state to be essentially degenerate as required for barrier free transitions during catalysis[1]. Further, product formation experiments demonstrated the effect of perturbing polar solvents on the electronic state of the catalyst producing reaction rates and polymer chain lengths dependent on presence of electron pair donors of the polar solvents. This data was unusually revealing contributing to understanding of catalytic polyethylene formation.

References

[1]. Carter, M.K. "Concepts of Catalysis", prepared for publication.
[2]. Carter, M. K. J. Molecular Catalysis A: Chemical 2001172, 193.
[3]. Carter, M. K. J. Molecular Catalysis A: Chemical2003200, 191.
[4]. The experimental work was conducted at Shell Development Company, Emeryville, CA in 1969. Participants who contributed to this project were Ron Bauer, Harold Chung, Joseph deMartino, Peter Glockner and Wiley Keim.
[5]. (a) Bauer, R. S., Chung, H., Glockner, P. W., Keim, W. and van Zwet, H., U.S. Patent number 3,644,563.
[6]. (b) Glockner, P. W., Keim, W. and Mason, R. F., U.S. Patent number 3,647,914.
[7]. (c) Bauer, R. S., Chung, H., Barnett, K. W., Glockner, P. W. and Keim, W., U.S. Patent number 3,686,159.
[8]. Bauer, R. S., Chung, H., Glockner, P. W., Keim, W. and van Zwet, H., U.S. Patent number
[9]. 3,635,937.
[10]. Shapiro, N. D. and Toste, F. D. "Synthesis and structural characterization of isolable phosphine coinage metal π-complexes" Published online before print February 19, 2008, doi:10.1073/pnas.0710500105 PNAS February 26, 2008 vol. 105 no. 8 2779-2782.
[11]. Bellamy, L.J. "The Infrared Spectra of Complex Molecules", Volume 1, 3rd Edition, Chapman and Hall, New York, 1975, p 359.
[12]. Peuckert, M. and Keim, W. Organometallics 2, 594-597, 1983.
[13]. Chandra, S., Raizada, S., Tyagi, M. and Gautam, A. Bioinorg. Chem. Appl. 51483, 2007;published online 2007 September 27. doi: 10.1155/2007/51483.
[14]. Cammack, R., Patil, D., Aguirre, R. and Hatchikian, E. C. FEBS Letters, 2, 142, 289-292, 1982.
[15]. Saraev, V. V. Kraikivskii, P. B. Matveev, D. A. Petrovskii, S. K. and Fedorov, S. V.
[16]. Published online: 10 September 2008; Original Russian Text published in Koordinatsionnaya
[17]. Khimiya, 2008, Vol. 34, No. 9, pp. 719–720.
[18]. Cotton, F. A. and Wilkinson, G. "Advanced Inorganic Chemistry", John Wiley & Sons, New York, 4th edition, 1980, pp 790-791.
[19]. Woodland, M.P.; Patel, D.S.; Cammack, R.; Dalton, H. Biochim. Biophys. Acta**1986**873, 237.
[20]. Rosenzweig, A.C.; Frederick, C.A.; Lippard, S.J.; Nordlund, P. Crystal Structure of a Bacterial non-haem Iron Hydroxylase that Catalyses the Biological Oxidation of Methane, Nature**1993**366, 537-43.
[21]. Bleaneyas found in "Paramagnetic Resonance", by GE Pake, Published by W.A. Benjamin, Inc., New York, 1962, pp 74-78.
[22]. Guo, Jing-ru, Wang, Ting-ting, Zhang, Zhao-xia, Chen, Cong-xiang and Chen, Yang
[23]. Chin. J. Chem. Phys.21, 308, 2008. doi: 10.1088/1674-0068/21/04/308-313.

M.K. Carter. "ESR Spectra Illuminate a Molecular Mechanism for Nickel(I) Catalysis of Ethylene Polymerization." *IOSR Journal of Applied Chemistry (IOSR-JAC)*, 13(5), (2020): pp 01-10.